World Academy of Science, Engineering and Technology
International Journal of Materials and Metallurgical Engineering
Vol:18, No:3, 2024

Investigating the Viability of Small-Scale Rapid Alloy Prototyping of Interstitial Free Steels

Talal S. Abdullah, Shahin Mehraban, Geraint Lodwig, Nicholas P. Lavery

***Abstract*—**The defining property of Interstitial Free (IF) steels is formability, comprehensively measured using the Lankford coefficient (r-value) on uniaxial tensile test data. The contributing factors supporting this feature are grain size, orientation, and elemental additions. The processes that effectively modulate these factors are the casting procedure, hot rolling, and heat treatment. An existing methodology is well-practised in the steel industry; however, large-scale production and experimentation consume significant proportions of time, money, and material. Introducing small-scale rapid alloy prototyping (RAP) as an alternative process would considerably reduce the drawbacks relative to standard practices. The aim is to finetune the existing fundamental procedures implemented in the industrial plant to adapt to the RAP route. IF material is remelted in the 80-gram coil induction melting (CIM) glovebox. To birth small grains, maximum deformation must be induced onto the cast material during the hot rolling process. The rolled strip must then satisfy the polycrystalline behaviour of the bulk material by displaying a resemblance in microstructure, hardness, and formability to that of the literature and actual plant steel. A successful outcome of this work is that small-scale RAP can achieve target compositions with similar microstructures and statistically consistent mechanical properties which complements and accelerates the development of novel steel grades.

***Keywords*—**Interstitial free, miniaturized tensile specimen, plastic anisotropy, rapid alloy prototyping.

I. Introduction

IF steel is heavily involved in the automotive and packaging industry purely because of its stamp-forming capabilities. Its excellent formability properties allow the thin sheet steel to be stamp formed into complex geometry car parts [1]. A good formability requires a clean ferritic matrix that is free from interstitial elements and defects that would hinder the overall formability of the material. Hoile [2] wrote a literature review on the processing and properties of IF steels and mentioned that IF steel is cast in a degassed vacuum chamber to support ultra-low C, < 30ppm, and low nitrogen, < 40ppm, within the melt. Removing the existing interstitial solutes from the matrix requires the addition of alloying elements, like Ti, to form precipitates.

$$Ti_{stab} = 4C + 3.42N + 1.5S \quad (1)$$

$$Ti^{*} = Ti_{total} - Ti_{stab} \quad (2)$$

Fekete et al. [3] stated that in Ti-stabilised IF steel, Ti reacts with C, N, and S to form TiN, TiS, TiC, and Ti(C+S); the amount of Ti needed to stabilise (Ti_{stab}) the ferritic matrix of the interstitials is displayed in (1). The equation assumes that the reaction is in equilibrium when that is not the case, and so excess Ti (Ti*), which is calculated using (2), is required to ensure that the precipitation reaction is complete. This reduces the inhibiting effect of producing preferred texture components associated with formability, which is the {111}. When Ti* is greater than 0.02wt.% the Lankford coefficient (r-value) begins to increase [3].

TABLE I
Units for Tensile Properties and Hot Rolling

Symbol	Quantity	Units
$Rp_{0.2}$	0.2% proof strength	MPa
Rm	Tensile strength	MPa
Ag	Uniform elongation	%
A_{10}	Elongation to failure	%
r-value	Lankford Coefficient	-
$r_{15\%}$	Lankford Coefficient at 15% elongation	-
$r,^{-}$	Mean Lankford Coefficient	-
n	Strain hardening exponent	-
K	Strength Coefficient	
$n_{5\text{-}10\%}$	Rate of strain hardening at 5 – 10% elongation	-
$n_{10\text{-}15\%}$	Rate of strain hardening at 10 – 15% elongation	-
$n_{10\text{-}20\%}$	Rate of strain hardening at 10 – 20% elongation	-
d_{max}	Maximum draft	mm
L	Contact Length	mm
α	Roll bite angle	°
Ar_3	Austenite → ferrite transformation temperature	°C
$T_{coiling}$	Coiling temperature	°C
l_{RD}	Mean intercept length for grain size	µm

To maximise the deep drawing quality of the material, it is paramount that the temperature is strictly controlled at exit during hot rolling whilst applying significant reductions to refine the ferritic grains. Coiling is then followed to facilitate sparse dispersions of coarse precipitates to reduce pinning effects during the strain-induced boundary migration (SIBM) and sub-grain growth during recrystallisation. Hutchinson [4] explains that the effects of pinning result from the fine precipitates populated around grain boundaries; this makes it harder to recrystallise the grains with higher stored energy texture components. Significant reductions are also necessary during cold rolling as it stores energy in the ferritic grains; the energy difference between neighbouring grains is a driving

T. S. Abdullah is with the Faculty of Science and Engineering, Bay Campus, Swansea University, SA1 8EN UK (corresponding author, phone: +447989072919; e-mail: 871857@swansea.ac.uk).
S. Mehraban and N. P. Lavery are with the Faculty of Science and Engineering, Bay Campus, Swansea University, SA1 8EN UK (e-mail: s.mehraban@swansea.ac.uk, n.p.lavery@swansea.ac.uk).
G. Lodwig is with the Product Management & Development, Tata Steel UK (e-mail: geraint.lodwig@tatasteeleurope.com).

force for SIBM. During annealing, the grains with maximum stored energy act as nucleation sites for birthing new grains that assume the {111} orientation. The lower the reduction in cold rolling, the lower the stored energy, which in turn reduces the intensity of the {111} component and increases the undesirable texture {001}.

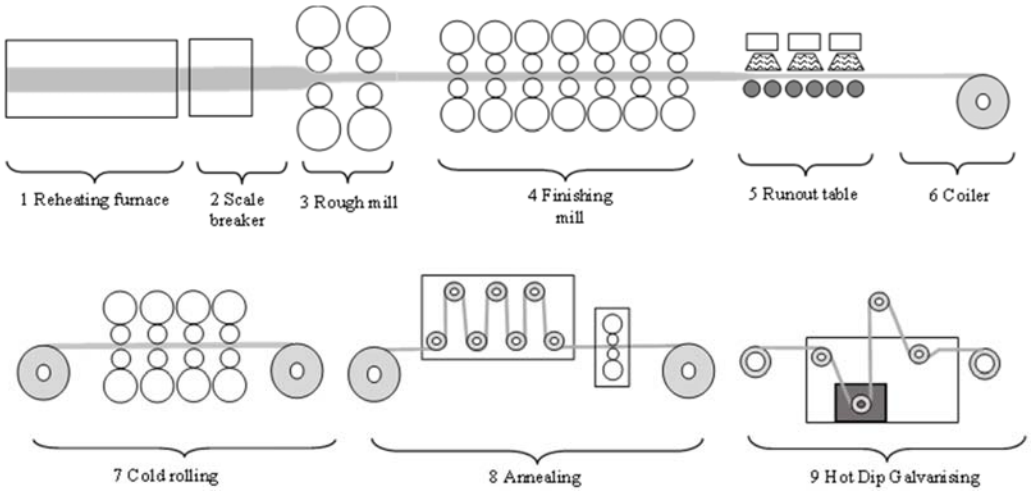

Fig. 1 Industrial production route of IF steel

Industrial production of IF steel, as shown in Fig. 1, involves continuous casting with a lean chemistry that includes predominantly Fe and micro additions of Ti, Mn, and Al. The hot slab is descaled and passed through the roughing mill at ~1160 ºC and experiences > 80% overall reduction across five passes, which breaks the cast structure and reduces the overall thickness of the material ready for the finishing mill. During the finishing mill process, the roughed slab experiences an overall ~89% reduction across several passes at high strain rates where the finishing rolling temperature (FRT), 910-960 ºC, is above the upper critical transformation temperature, Ar_3. Vanderschueren et al. [5] reported that the FRT of the studied IF steel, with chemistry in Table II, is 920 ºC. Tsunoyama [6] explained that the typical hot rolling processing conditions for ultra-low carbon IF steels are for the FRT to be above the Ar_3, which ensures that all the austenite grains completely recrystalise into the ferrite. The hot band strip is then coiled at 710 ºC. Once the coiled strip has reached room temperature, it is cold rolled, experiencing an 82% reduction, bringing the final gauge thickness to 0.7-0.8 mm. Lastly, the process finishes with an annealing cycle, where the soak temperature is 820 ºC, and a hot-dip galvanising for coating.

RAP is a relatively new steel production and testing process that entails working with considerably small quantities of materials ranging from 20 g to 30 kg. Working with steel of such small masses allows for a speedy process throughout the full processing chain. The elemental additions are weighed and melted sequentially to avoid contamination or excessive oxidation. Lavery et al. [7] demonstrated the turnaround of the RAP process by completing the through production of 60 steel compositions in 2-3 weeks, averaging at 2 hours per sample. The author proved that the RAP process can accelerate the compositional studies to approximately 6-9 times quicker than conventional practices. Farrugia et al. [8] articulated the establishment of four different RAP lines operating in the UK to link the small-scale process with the big-scale; the 20-40 g and 200 g (Materials Advanced Characterisation Centre, University of Swansea), 4.5 kg (WMG, University of Warwick), and 30 kg (Steel and Metals Institute, University of Swansea) routes. Depending on the mass of the material, there are various melting/casting RAP lines. In the 20 g-80 g RAP route, the material is melted in a CIM glovebox machine; in a larger 140 g route, the material is melted in a centrifugal casting machine; > 10 kg is melted in a vacuum induction melting machine (VIM). The authors collaborated to benchmark industrial DP-grade steel production, characterisation, and mechanical testing via the RAP route.

In the 20-40 g and 200 g routes, there is sufficient material at the end of the process: hot rolling, cold rolling, and annealing, to support the fabrication of up to five ASTM25 tensile bars. Yar et al. [9] took the 40 g coil induction RAP process to explore the effects of Cu and Cr residuals in extra-low carbon steel. At the end of the process, a 12 x 230 mm strip can provide enough material to fabricate three ASTM25 bars in the length direction. The authors were able to map a trend in mechanical properties. To ensure repeatability in the mechanical properties of a single strip, designs of smaller bars are necessary. Zhang et al. [10] designed non-standard miniaturised tensile specimens (MTS) suitable for attaining appropriate repeats from 20-40 g and 200 g strips of the following steel grades: DP800, DP600, and 316L stainless steel. Zhang et al. [11] carried out a supplementary study on the influence of aspect ratio on the necking angle when scaling down tensile specimens to further ensure confidence in the new designs. Abdullah et al. [12] continued the study of MTS but on IF steel and observed scaling effects and concluded observable effects when measuring the uniform elongation, *Ag%*, total elongation, *A%*, rate of strain hardening, $n_{10\text{-}15\%}$ and $n_{10\text{-}20\%}$, and the plastic anisotropy r-value, $\bar{r}$-value. The stress values (0.2% proof strength, $Rp_{0.2\%}$, tensile strength, *Rm*) from the MTS were unaffected. Furthermore, the

author concluded that the Mini1 (10 mm gauge length) was the MTS for measuring the mechanical properties, especially for the plastic anisotropy r-value. The Mini2 (5 mm gauge length) specimen brings about significant scatter. Zhang et al. [13] explored to the feasibility of using MTS predict the total elongation and formability behaviour of DP800 and DP600. The authors discovered that the forming behaviour of the dual phase alloys, produced from the RAP_{40g} process, can be predicted with confidence with the mini1 being the most suitable of the MTS. Zhang et al. [14] did a study on the post-necking behaviour of the and developed a model to understand further how the MTS deforms post the Rm. The triaxiality increased earlier and slower for the MTS, which has aspect ratios of 1.67-2.5.

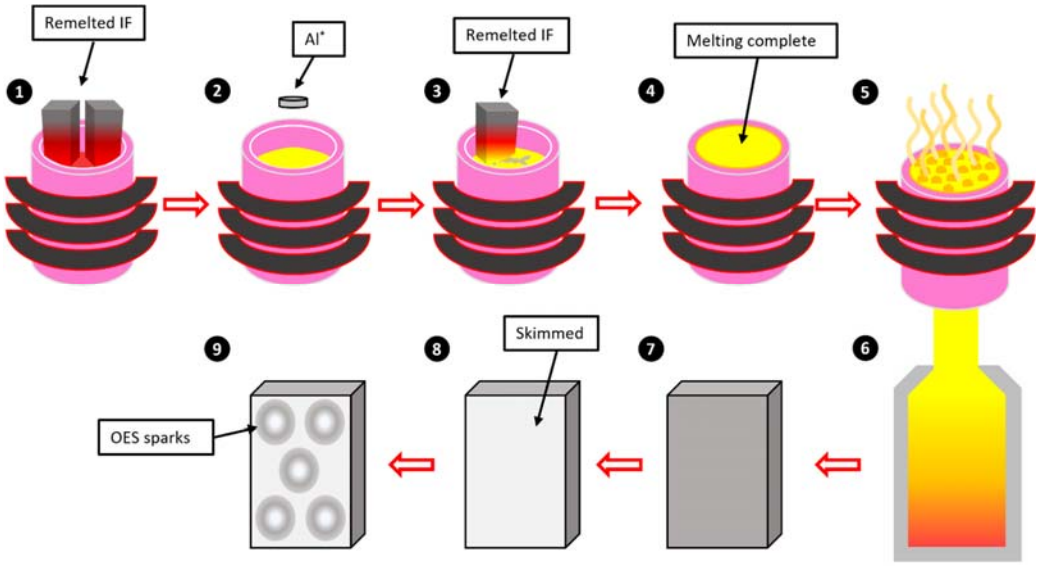

Fig. 2 The $RAP_{20\text{-}80g}$ CIM process for remelting IF steel, where the ULC IF material is remelted with Al* (steps 1-4), drop-casted in to a BN mould (steps 5 and 6), air-cooled (step 7), skimmed on both surfaces (step 8), lastly measured for composition using the OES (step 9)

TABLE II
CHEMICAL COMPOSITION OF IF STEEL (WT.%)

Source	Reference	C	Si	Mn	P	S	N	Al	Ti	Ti*
BS EN 10346	[15]	< 0.12	< 0.50	< 0.60	< 0.10	< 0.045	-	-	< 0.300	-
Vanderschueren	[5]	0.0019	0.010	0.130	0.014	0.014	0.0026	0.041	0.046	0.009
Hoile	[2]	< 0.003	0.025	0.150	0.017	0.012	< 0.004	-	> 0.040	> 0.020
Kobayashi	[16]	0.0021	0.0014	0.143	0.0046	0.0045	0.0022	0.033	0.045	0.022

In the 20 g-80 g route, the melt is drop-casted into a BN mould with an inner shape of a rectangular block [9]. Reheating is carried out in a preheated box furnace at 1250 ºC for 5 minutes and then subjected to hot rolling. Retaining the temperature post-reheating is impossible once exposed to ambient air; due to the size of the cast, heat loss experienced is rapid, so the transition from reheating to hot rolling must be uninterrupted. This case also makes it difficult to induce multiple hot deformation passes onto the material, especially if FRT is required to be high. Further processing steps, such as coiling, cold rolling, and annealing, can also be carried out depending on the grade of the material. The challenges with IF grade steels include being able to control the tight processing condition from compositional weight % to narrow processing windows for processing temperatures and reheating/cooling rates during annealing.

This paper explores the RAP production of IF steel using remelted industrial feedstock to determine whether small-scale production and mechanical testing are viable ways of generating the fundamental metallurgical and mechanical properties of a material that is representative of the industrial made hot band. Considering the FRT must be above the Ar_3, which is reported to being 890-920 ºC [17], [18], all the reductions must be experienced in a single pass to avoid falling below the critical temperature. The hot band microstructure should be homogeneous, equiaxed, and have a mean grain size of 10-20 µm. The mechanical properties of the remelted IF steel will be determined by tensile testing MTS, Mini1 (Fig. 4), developed by Zhang et al. [10], as the size of the material does not support the fabrication of standard tensile geometries: e.g., BS EN ISO 6892-1 [19] standard A80 and A50.

II. PRODUCTION AND TESTING METHOD

A. Material

The chemical composition of the ultra-low carbon (ULC) IF steel, to be cast, must abide by the BS EN 10346 [15] standard targets found in Table II. The maximum allowable compositional limits are outside the tolerance of ULC IF steel, so it is necessary to constrain the composition to the limits of a ULC deep-drawing quality steels [2]. This grade of steel has an entirely body centred cubic (bcc) ferritic matrix with

precipitates, such as: TiN, TiS, TiC, and Ti(C+S) scattered in and outside of the grain boundaries.

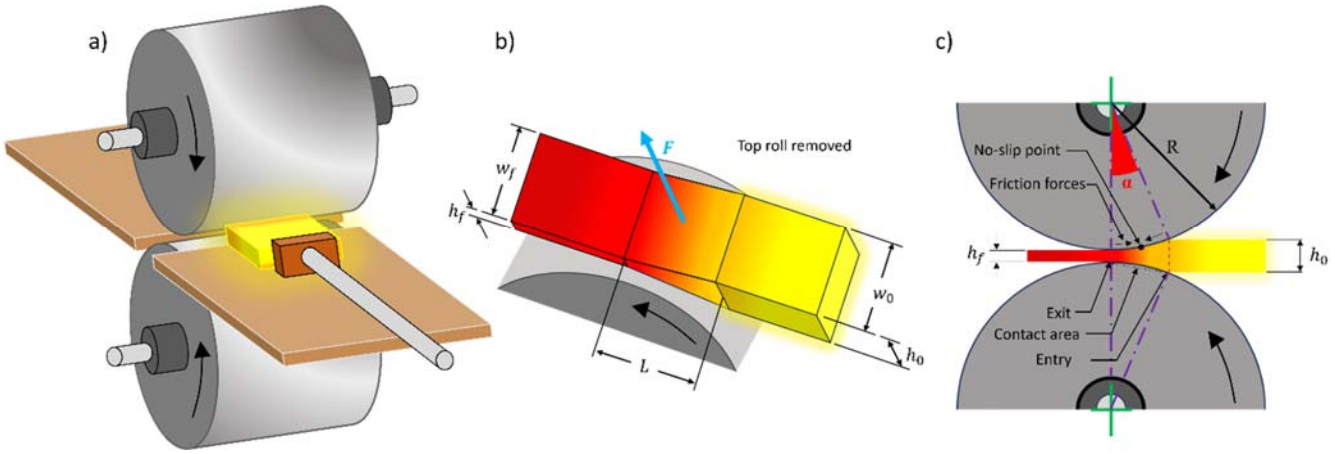

Fig. 3 Illustration of the finishing mill where (a) is a trimetric view of how the reheated sample is fed in to the rolls; (b) is a trimetric view of the sample passing through the rolls with the annotations original height, h_0, original width, w_0, final height, h_f, final width, w_f, force, F, and contact length, L; (c) is a side cross-sectional view of the rolls showing the bite angle

B. Coil Induction Melting

The material is prepared by weighing out 80 grams of ULC IF steel and the micro addition of excess Al to compensate for the loss during melting. Once all the material is weighed, the melting process, as depicted in Fig. 2, is carried out in the CIM glovebox machine, which consists of a sequence of remelting blocks of ULC IF steek and excess Al (Al*) within an Al_2O_3 crucible. Thorough mixing of the melt is possible due to the fluctuating magnetic fields induced by the coils, which is essential for a homogenous distribution of the chemistry; it is then drop-cast into a BN mould. The dimensions of the casting are 35 x 25 x 10 mm. To accurately measure the material's composition, the top and bottom surface of the As-cast block is skimmed and then measured on the Optical Emission Spectroscopy (OES) and LECO for more accurate C wt.% and S wt.%.

C. As-Cast Reheating

The As-cast ingot is reheated to an austenitic temperature of 1250 °C in a preheated box furnace for 5 minutes in preparation for hot-rolling. High reheating temperature is necessary to account for extreme temperature losses during the transition period from reheating to hot rolling. Most precipitates are in solution; however, TiN is very stable even at the set reheating temperature [2], so they are not expected to change throughout the entire line production.

D. Hot Rolling and Coiling

During the reheating of the As-cast ingot, scale accumulates at the surface. Consequently, a descaling procedure was implemented to prevent roughening of the hot band surface and non-uniformity of the thickness along the strip caused by the embedded fractured scale. The descaled ingot is then fed into the hot rolls, where maximum reductions are imparted at the maximum strain rate of the mill. Pyrometers on both sides of the rolls record the entry and exit temperatures. The small-scale hot rolling mill is suitable for deforming ingots of mass 20-200 g. In the RAP_{80g} route, there are limitations to how much reduction the material can undergo in a single pass.

$$d_{max} = \mu^2 R \tag{3}$$

$$L = \sqrt{R(h_0 - h_f)} \tag{4}$$

$$\alpha = tan^{-1}\left\{\frac{L}{\left(R-\frac{h_0-h_f}{2}\right)}\right\} \tag{5}$$

The maximum draft, d_{max}, can be calculated using (3) if the coefficient of friction, μ, is known. An alternative way is to apply significant reductions on to the strip, if the final gauge is considerably less than the target gauge then the d_{max} is found, 7 mm. Hence, a maximum reduction of 70% can be achieved in a single pass for a strip with an initial height, h_o, of 10 mm. The front edges of the chamfered strip must at least be in contact with the roll bite angle, α, 23°, calculated using (4) and (5) [20]. This reduction will yield a hot band strip with dimensions 40 x 78 x 3 mm, as depicted in Fig. 5. The exit temperature must be above and close to the Ar_3, which is 890-920 °C [17], [18]. In the industrial process, a run-out table would then follow to control the cooling of the hot band strip before coiling, which is at 710 °C. However, in the small-scale route, the sample is placed into the second box furnace set to 710 °C and then furnaced cooled to allow for slow cooling rates to simulate the effects in the coiling process.

E. Mechanical Testing

Tensile testing is used to acquire the mechanical properties. An MTS, Mini1 (Fig. 4), was machined from the hot band strips in the rolling direction (RD), as shown in Fig. 5. The MTS used is the mini1, allowing for three repeats per strip as it has a gauge length (L_o) of 10 mm and total length (L_t) of 40 mm as shown

in Fig. 4. By following Oliver's law, decreasing specimen size has an impact on the *A%* of the material. A previous study [12] has shown that it is necessary to quantify the scaling effects of the IF material cold-rolled + annealed industrial material to ensure that MTS is representative of the standard specimen results. Due to the size constraint of the hot band strip, standard specimens cannot be machined to carry out such a study.

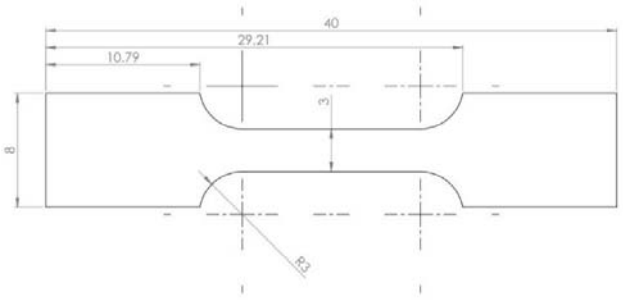

Fig. 4 Engineering drawing of the Mini1 tensile specimen; the measurements are in 'mm'

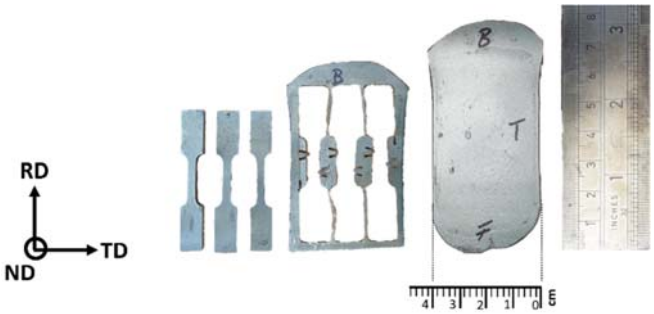

Fig. 5 Mini 1 tensile bars (Fig. 4) machined from hot band strip with dimensions 40 (W) x 78 (L) x 3 (T) mm

Considering the study required capturing both the transverse and longitudinal strain of a miniaturised specimen, video extensometers offer benefits over traditional mechanical clip-on extensometers. As shown in Fig. 6, the video extensometer tracks the pixels associated with the measuring points of interest and computes the strain values. The strain rates follow a known standard, irrespective of the specimen being of a non-standard geometry; Abdullah et al. [12] demonstrated that the standard strain rates are acceptable for the Mini1 tensile geometry. The BS EN ISO 6892-1 [19] standard uses two strain rates, range two at 0.015 min^{-1}, which occurs from the start of the tensile test to the end of the 0.2% proof strength ($Rp_{0.2}$), and range four at 0.4 min^{-1}, which begins straight after the $Rp_{0.2}$ and continues until fracture.

F. Profilometry-Based Indentation Plastometry

Profilometry-based Indentation Plastometry (PIP) is a technique that involves deriving a material's stress-strain curve from an indentation profile through accelerated inverse finite element analysis [21]. PIP performs an indentation with a predetermined load to achieve a specified depth. Employing a rigid, spherical indenter, it generates an indentation approximately 100-200 µm in depth and around 1 mm in diameter. This indentation size is greater than those produced in nanoindentation or hardness tests, indicating that the indentation is more of a reflection of bulk material than opposed to individual grains. Subsequently, the built-in profilometer examines and records the residual shape of the indentation profile. Commencing with an initial set of plasticity parameters, a finite element simulation of the indentation is executed. A subsequent assessment is conducted by contrasting the modelled indentation profile with the actual measured profile. The plasticity parameters are refined through an iterative process until optimal alignment between the profiles is attained. These plasticity parameters establish a connection to the stress-strain curve through a constitutive equation, serving as a descriptor for the plastic behaviour. This technique requires initial input values that assume the general property of the material tested; for instance, Young's modulus is fixed at 200 MPa for steel. A minimum sheet thickness of 1–1.5 mm makes it acceptable for use on hot band material.

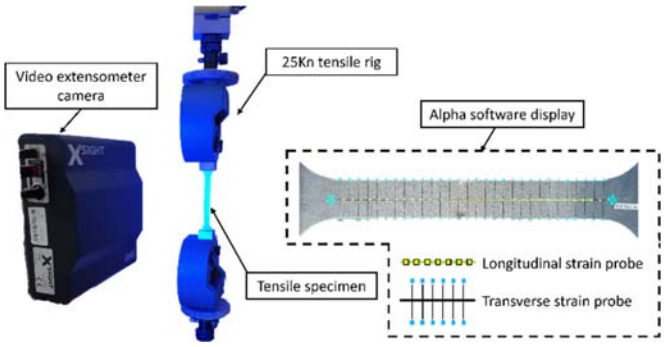

Fig. 6 Illustration of the 25 kN tensile rig set up with a video extensometer and a snippet of the display screen from the Alpha software program which measures the change in width and length by using longitudinal and transverse probe points to track the movement of the pixels

G. Microscopy and Hardness

Sample preparation is required to study microstructure. The specimen sectioned in the RD direction is first mounted in a conductive powder called Bakelite. The mounted sample goes through various surface roughness discs and polishing steps using MetaDi diamond suspension: 9 µm, 6 µm, and 1 µm. The final step requires etching with 2% Nital solution to reveal the ferritic grains, which will be observed on the optical microscope. The scanning electron microscope (SEM) coupled with energy dispersive spectroscopy (EDS) allows for compositional analysis of a highly magnified area of interest in the sample. The hardness machine measures a material's hardness (HV) by taking a preprogrammed matrix of indents (2 x 5). This technique has merit as it allows the flexibility to observe hardness variation across the dimensional limits of the work specimen.

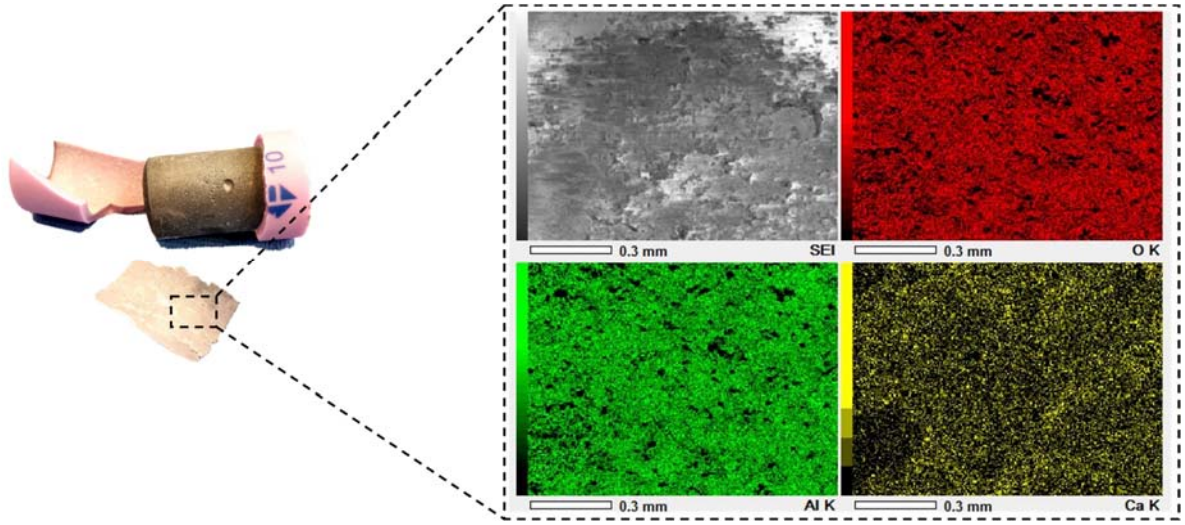

Fig. 7 EDS can of the flake layer found between the crucible and the As-cast material

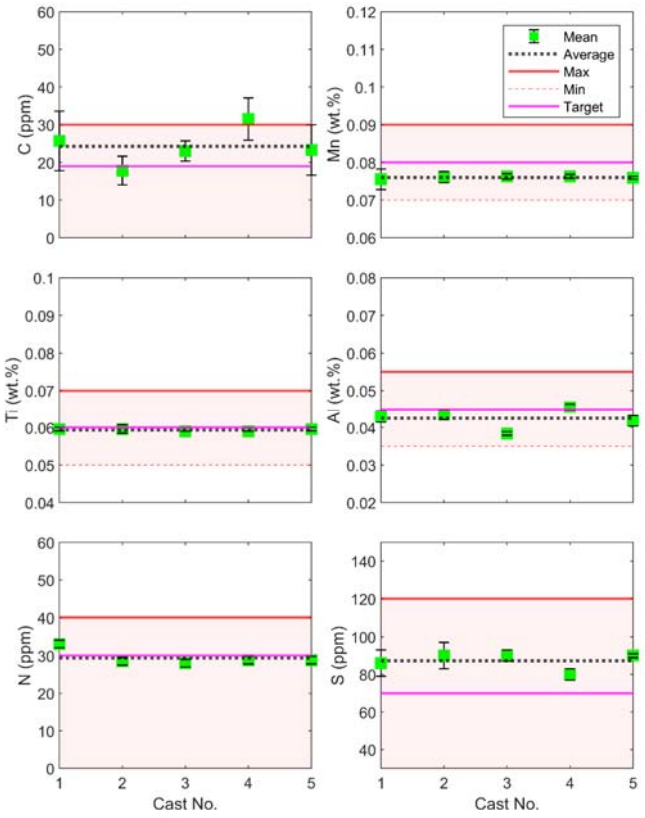

Fig. 8 Composition accuracy of C, Mn, Ti, Al, N, and S, where the five casts are repeats of remelted 80 grams of IF material from the industry

III. Results and Discussion

A. Compositional Control

Loss of Al

To understand how much Al is lost post-casting, three casts with intended varying excess Al are added during the RAP_{80g} melting/casting process. An average of 0.0215 wt% of Al was lost; therefore, the same amount is required as excess addition to meet the target level of 0.045 wt.% Al.

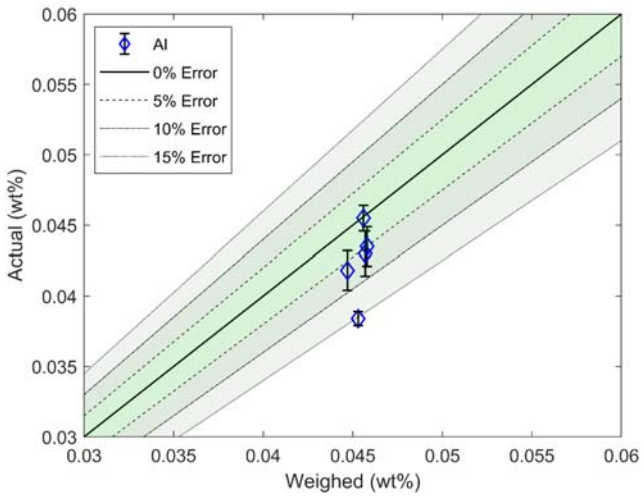

Fig. 9 Compositional accuracy of Al, comparing the actual wt% measured by OES to the weighed wt%

EDS Analysis of Al_2O_3

Relatively considerable amounts of aluminium are lost from the melt due to oxidation. A thin flake layer was found between the cast and the crucible, sampled, sectioned and placed into the SEM for EDS analysis. Fig. 7 shows the scan images from the EDS; the analysis showed a dominating concentration of Al, 60.72wt%, and O, 33.92wt%. Equation (6) is the reaction equation for Al_2O_3, where it consists of 52.9% mass of Al and 47.1% mass of O. Although the results are not identical, the formation of Al_2O_3 is the most convincing explanation for the partial absence of Al.

$$Al_2O_3 \rightarrow 52.9\%Al + 47.1\%O \quad (6)$$

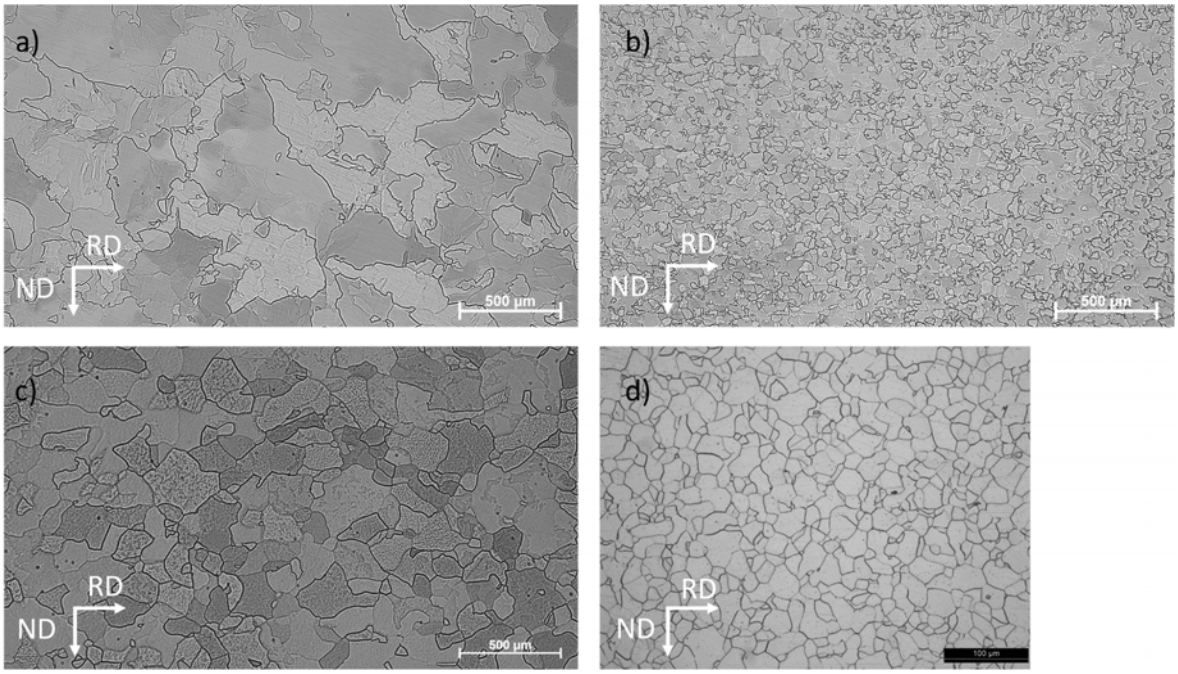

Fig. 10 Optical microscope images of the microstructure before the finishing mill, (a) and (c), and after the finishing mill and coiling, (b) and (d); the top row are images of the RAP_{80g} remelted IF, where (a) is the as-cast microstructure, and the bottom row are images of the industrial IF material, where (b) is the transfer bar material produced after the roughing (cogging) schedule

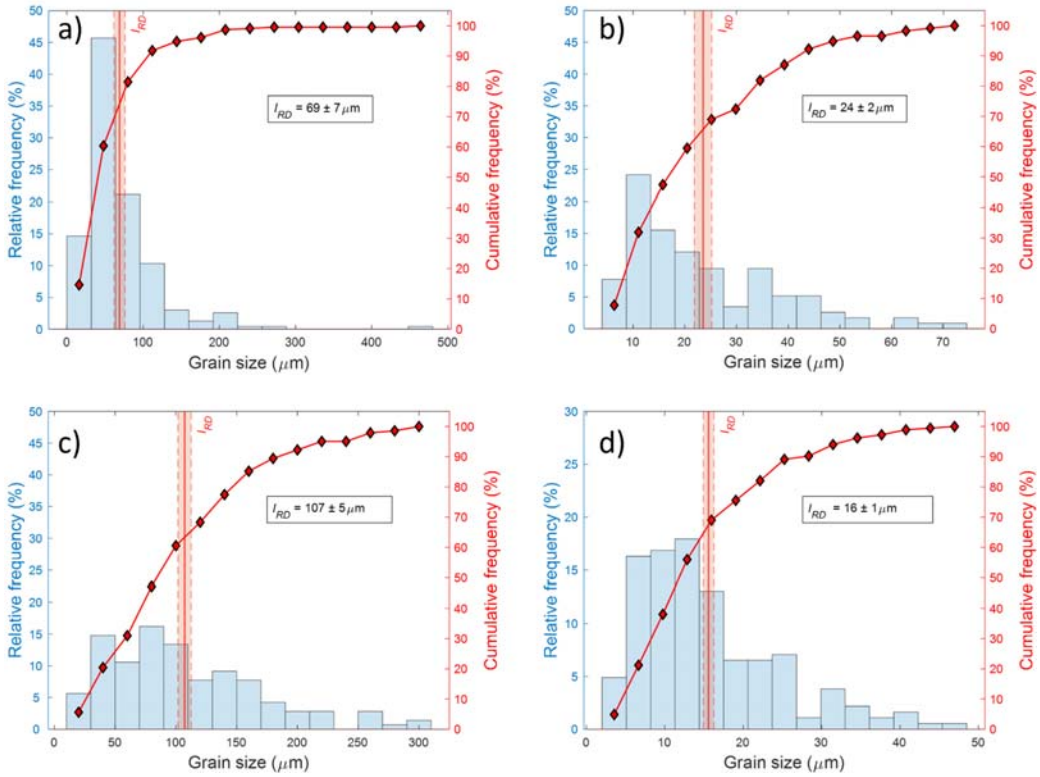

Fig. 11 Histogram of the grain size distributions with a display of the relative frequency (%) and cumulative frequency (%). The order of the histograms follows the same order as in Fig. 10

Compositional Accuracy of C, Mn, Ti, Al, N, and S

In Fig. 8, the repeatability of the elemental compositions is demonstrated across five casts with the same predetermined target chemistry. Each cast has ten OES sparks in line with the OES standard [22], giving an average of the wt.% of each element presented as the error bars. The success of the melting

procedure is verified based on whether the measurements are within the set tolerances, which for C, N, and S, are found in Table II [2], and Mn, Ti, and Al were set to ± 0.01 wt.%. It is evident that the Al has the most variation, which may be because of the varying oxygen content within the electrolytic iron flakes per batch used to produce the 40 g casts. Nonetheless, the predicted wt.% of Al* required to purge the oxygen from the melt, produced casts where the Al wt.% is within the acceptable tolerance. The average Al wt.% across the five casts is 0.0475 wt.%, a ~6% difference, and the relative standard deviation (RSD) is 11%. The maximum C variation amongst the casts is ± 8 ppm, within the acceptable tolerance of the ultra-low C standard used to calibrate the machine. The mean C measurement is within the tolerance, its mean average is 5 ppm higher than the target, and the RSD is 20%. Due to the small quantity of C, the RSD is expected to be more sensitive. Most of the C is from the electrolytic Iron flakes.

Moreover, Mn gave the best repeatability with an RSD of 2%; the mean Mn wt.% was also identical to the target. The variation of Ti readings per cast was across all the elements, the overall average wt.% was 7% lower than the target, and the RSD was 5%. This demonstrates that the chemical composition's repeatability is possible across the elements presented, which will help when carrying out a study on the effects of a particular element that is to be varied by small increments of wt.%. Additionally, the chemistry is in accordance with the BS EN 10346 standard (Table II) [15].

The comparison between the weighed composition and the actual composition is displayed in Fig. 9 with %error limits. Al is spread across the range 0 > %error ≥ -15, as the amount of Al needed to be compensated due to oxidation was fixed, when in fact it varies. In some instances, there may be slightly more O and in others, slightly less.

B. Hot Rolling

1) Microstructure Analysis Pre and Post Finishing Mill and Coiling

In Fig. 10, a display of micrographs is used to show the effects of carrying out the finishing mill process on the RAP80g route (Figs. 10 (a) & (b)) in comparison to the industrial process (Figs. 10 (c) & (d)). Grain size analysis was carried out on the images to assess the level of grain refinement (Fig. 11). Fig. 10 (a) is a micrograph of the as-cast material with a l_{RD} of 69 ± 7 µm. Fig. 10 (b) is a micrograph of the hot band after imparting the maximum reduction (70%) in a single pass during the finishing mill; it has a l_{RD} of 24 ± 2 µm. Fig. 10 (c) is a micrograph of the industrial transfer bar material with a l_{RD} of 107 ± 5 µm. Fig. 10 (d) is a micrograph of the industrial hot band after imparting > 80% reduction across seven passes during the finishing mill; it has a l_{RD} of 16 ± 1 µm. The difference in the grain sizes between the two routes is simply due to the 19% difference in the reduction and the significant difference in the strain rate. The industry uses strain rates that reach > 100 s^{-1} [23], whereas the small-scale rolling mill for the RAP_{80g} has a maximum strain rate of ~6 s^{-1}.

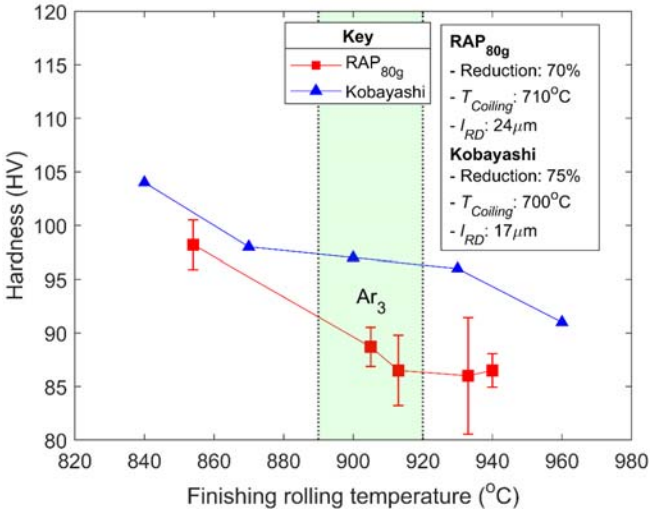

Fig. 12 Hardness (HV) vs FRT (°C) comparison between the RAP_{80g} and IF study carried out by Kobayashi [16]

2) Hardness vs FRT

As mentioned earlier, the FRT must be above but near the Ar_3 to maximise the grain refinement and sparse dispersion of coarse precipitate potential. One of the variant ways of studying the effects of the FRT on the microstructure is by undertaking hardness testing on the hot band samples. For the RAP_{80g} route, the maximum reduction that could impart onto the cast material was 70%. Considering the reduction is not to industrial levels (> 80%), the grains are expected not to be as refined. Five hot rolling schedules were carried out, where the FRT ranged from 940 °C, above the Ar_3, to 854°C, below the Ar_3 [17], [18]. They were both then followed by coiling at 710 °C. Each sample was then measured for hardness. In Fig. 12 the hardness value can be seen to increase sharply by 10HV when the FRT is below the Ar_3 relative to when it is slightly above the Ar_3. It is understood that smaller grains yield higher hardness and contrariwise. However, it is essential to note that any rolling below the Ar_3 induces stress into the ferritic grains causing them to be pancaked as it accumulates the strain. Therefore, the higher hardness could also indicate how much strain has been accumulated into the ferritic matrix. Kobayashi [16] carried out a study on the effects of FRT on the microstructure's hardness, which showed similarities with the RAP_{80g} study. The author conducted research on an IF steel with chemistry listed in Table II. As shown in Fig. 12, the hardness value increases with decreasing FRT. The difference in hardness values at 900 °C and 840 °C is 7HV. The author has higher Hardness results due to the 75% reduction imparted to the material; it will produce finer grains if all conditions are fixed. However, as a study on the trend, the similarities are evident.

C. Tensile Testing

1) Hot Band Tensile Properties vs FRT

Although the main interest of the hot band material is the grain size, it was intriguing to explore the material's tensile properties and compare it to the results measured from the

Profilometry-based Indentation Plastometry (PIP). Fig. 13 shows a stress-strain graph acquired from MTS specimens, Mini1. As hot band is an intermediate product, its mechanical properties are not generally reported in the literature; however, Interestingly, the Rm is already achieved, where the product of IF steel, post cold rolled and annealed, is expected to be ~300 MPa [12]. The formability displayed in the elongation is also evident, suggesting significant refinement of the grains. The average A% is 58% when the FRT is above the Ar_3 at a reduction of 70%. It should be considered that scaling effects apply to MTS, so it is necessary to determine the scaling constants using Oliver's Law to get a more representative value of the elongation related to the bulk material. Due to the limitations of the RAP80g hot band size, and lack of available hot band tensile test data, it is impossible to carry out a scaling effects study.

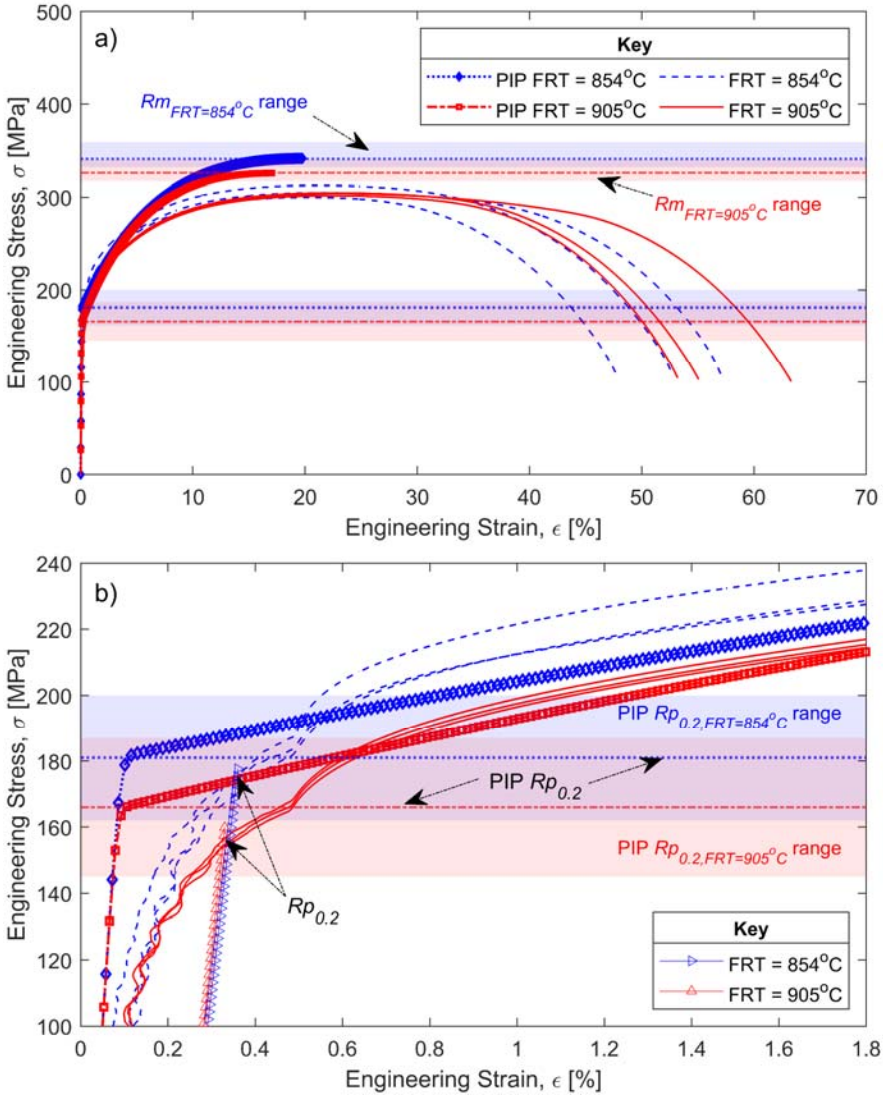

Fig. 13 Stress (σ) – strain (ε) curves of hot rolled tensile tests done on a MTS Mini1 (Fig. 4); profilometry-based Indentation Plastometry (PIP) results of the 0.2% proof strength, $Rp_{0.2}$, and tensile strength, Rm, are displayed as horizontal lines with the limits shaded and in the respective colour representing the data from the hot rolled strip with FRT of 854 °C (blue) and 905 °C (red)

It would be efficient and effective to use the PIP to predict the tensile properties of the hot band as a replacement for tensile testing if the %error relative to the tensile test data is acceptable. This would, as a result, preserve the material for further processing. As shown in Table III, the $Rp_{0.2}$ hot band strip with FRT 854 °C from the tensile test and PIP is 175 MPa and 181 MPa, respectively, giving a %error of 3%. The $Rp_{0.2}$ hot band strip with FRT 905 °C from the tensile test and PIP is 155 MPa and 166 MPa, respectively, giving a %error of 7%. The Rm of the hot band strip with FRT 854 °C from the tensile test and PIP is 306 MPa and 341 MPa, respectively, giving a %error of 10%. The *Rm*, when the FRT 905 °C, from the tensile test and PIP is 303 MPa and 326 MPa, respectively, giving a %error of 7%. This shows that the PIP over-predicts strength values by only 3 – 10%. The PIP appears to predict the $Rp_{0.2}$ more accurately than the *Rm*. According to Campbell et al. [24], PIP overpredicts the *Rm* for steel and Al metals. In addition, PIP is unreliable for measuring $n_{(5\text{-}10\%)}$ and $n_{(10\text{-}15\%)}$. Nonetheless, this

form of characterisation can prove helpful in predicting the strength values when factoring in the %error. The r-value for the hot band is low, ~1.1, which is expected, as the preferential texture is drastically influenced by the reductions imparted during cold-rolling Further work can be done to establish correction factors for the *K* and *n* derived from the PIP.

TABLE III
COMPARING THE PIP AND MTS TENSILE PROPERTIES OF HOT BAND WITH FINISHING ROLING TEMPERATURE ABOVE AR_3

FRT (°C)	Test	*K* (MPa)	*n* (-)	$Rp_{0.2}$ (MPa)	*Rm* (MPa)	*Ag* (%)	A_{10} (%)	$n_{(5\text{-}10\%)}$ (-)	$n_{(10\text{-}15\%)}$ (-)	$n_{(10\text{-}20\%)}$ (-)	$r_{15\%}$ (-)
854	Mini1	499 ± 15	0.186 ± 0.005	175 ± 6	306 ± 6	21 ± 1	53 ± 5	0.210 ± 0.004	0.203 ± 0.002	0.200 ± 0.002	1.16 ± 0.04
	PIP	605	0.237	181	341	20	-	0.292	0.257	-	-
905	Mini1	517 ± 2	0.210 ± 0.001	155 ± 3	303 ± 2	23 ± 0	58 ± 5	0.237 ± 0.001	0.223 ± 0.001	0.218 ± 0.001	1.09 ± 0.07
	PIP	595	0.240	166	326	17	-	0.282	0.218	-	-

IV. CONCLUSION

This paper has demonstrated the RAP_{80g} capability in producing and processing IF steel hot band by comparing it to the literature and known standards. Through remelting IF material using CIM process, tight compositional tolerances were met for C, N, S, Mn, Al, and Ti, moreover, it complies with the standard for IF steel. Due to the limitation in maximum reduction in a single pass, a grain refinement to 24 µm was possible. Further refinement can be achieved by adding a chamfer, that will comply with the bite-angle of 23°, on to the feed of the As-cast block. High elongation to failure values, 53-63%, were attained, which is an indication of the lean chemistry and degree of grain refinement carried out during hot rolling. Hardness increased with decrease in FRT, which was concurrent to what was found on a similar study. The 0.2% proof strength and tensile strength was achieved without taking the material through further processing. The hot band yielded an expected low Lankford coefficient r-value of 1.08, which enforces the need for cold-rolling and annealing. Profilometry-based Indentation Plastometry is a useful technique to predict the 0.2% proof strength with 3-7% error relative to the MTS data. Further work can be done to establish correction factors for the *K* and *n* derived from the Profilometry-based Indentation Plastometry to yield representable tensile strength and elongation values.

ACKNOWLEDGMENT

The author would like to thank Tata Steel UK, Welsh European Funding Office for the funding that made this research possible through the Materials and Manufacturing Academy (M2A Coated). The author would also like to acknowledge the EPSRC-funded Prosperity Partnership project, which has placed the context of this work in Rapid Alloy Prototyping. Thanks also must be given to the Welsh Government, European Regional Development Fund (ERDF), and SMART Expertise Wales for funding the equipment and technical staff of the Materials Advanced Characterisation Centre (MACH1) laboratory in which this work was done.

REFERENCES

[1] Rana R, Bleck W, Singh SB, Mohanty ON. Development of high strength interstitial free steel by copper precipitation hardening. Materials Letters. 2007; 61(14–15):2919–22. https://doi.org/10.1016/j.matlet.2006.10.037.

[2] Hoile S. Processing and properties of mild interstitial free steels. Materials Science and Technology. 2000; 16(10):1079–93. https://doi.org/10.1179/026708300101506902.

[3] Fekete JR, Strugala DC, Yao Z. Advanced sheet steels for automotive applications. JOM. 1992; 44(1):17–21. https://doi.org/10.1007/BF03222745.

[4] Hutchinson WB. Development and control of annealing textures in low-carbon steels. International Metals Reviews. 1984; 29(1):25–42. https://doi.org/10.1179/imtr.1984.29.1.25.

[5] Vanderschueren D, Yoshinaga N, Koyama K. Recrystallisation of Ti IF Steel Investigated with Electron Back-scattering Pattern (EBSP). ISIJ International. 1996; 36(8):1046–54. https://doi.org/10.2355/isijinternational.36.1046.

[6] Tsunoyama K. Metallurgy of Ultra-Low-C Interstitial-Free Sheet Steel for Automobile Applications. Physica Status Solidi (a). 1999; 167:427–33.

[7] Lavery NP, Mehraban S, Pleydell-Pearce C, Brown SGR, Jarvis DJ, Voice W, et al. Combinatorial development and high throughput materials characterisation of steels. Ironmaking and Steelmaking. 2015; 42(10):727–33. https://doi.org/10.1179/0301923315Z.000000000419.

[8] Farrugia D, Brown S, Lavery NP, Pleydell-Pearce C, Davis C. Rapid Alloy Prototyping for a range of strip related advanced steel grades. Procedia Manuf, vol. 50, Elsevier B.V.; 2020, p. 784–90. https://doi.org/10.1016/j.promfg.2020.08.141.

[9] Yar MA, Norrish C, Cullen JCT, Zhang L, Brown S, Underhill R, et al. Small-Scale Rapid Alloy Prototyping of Extra-Low Carbon Steel to Investigate the Effects of Cu and Cr Residuals. Minerals, Metals and Materials Series, Springer Science and Business Media Deutschland GmbH; 2022, p. 1202–13. https://doi.org/10.1007/978-3-030-92381-5_114.

[10] Zhang L, Harrison W, Yar MA, Brown SGR, Lavery NP. The development of miniature tensile specimens with non-standard aspect and slimness ratios for rapid alloy prototyping processes. Journal of Materials Research and Technology. 2021; 15:1830–43. https://doi.org/10.1016/j.jmrt.2021.09.029.

[11] Zhang L, Harrison W, Yar MA, Brown S, Lavery N. Influence of aspect ratio (AR) on the necking angle of tensile specimens for different alloys. 2nd International Workshop on Plasticity, 2021.

[12] Abdullah TS, Zhang L, Evans P, Lodwig G, Lavery NP. Scaling effects in miniaturised tensile testing on mechanical properties and plastic anisotropy r-values in Interstitial Free Steel 2023. https://doi.org/https://dx.doi.org/10.2139/ssrn.4399446.

[13] Zhang L, Harrison W, Yar MA, Mehraban S, Brown SGR, Lavery NP. Use of miniaturized tensile specimens to evaluate the ductility and formability of dual phased steels for Rapid Alloy Prototyping. Materials Science and Engineering: A. 2023; 875:145075. https://doi.org/10.1016/j.msea.2023.145075.

[14] Zhang L, Harrison W, Mehraban S, Brown SGR, Lavery NP. Size Effect on the Post-Necking Behaviour of Dual-Phase 800 Steel: Modelling and Experiment. Materials. 2023; 16(4):1458. https://doi.org/10.3390/ma16041458.

[15] BS EN 10346:2015 - TC. Continuously hot-dip coated steel flat products for cold forming. Technical delivery conditions. BSI; 2015.

[16] Kobayashi H. Microstructure Development in Ti Bearing Interstitial Free Steel with Simulated Hot Rolling Practice. ISIJ International. 1992; 32(7):873–81. https://doi.org/10.2355/isijinternational.32.873.

[17] Najafi-Zadeh A, Yue S, Jonas JJ. Influence of Hot Strip Rolling Parameters of Austenite Recrystallization in Interstitial Free Steels. ISIJ International. 1992; 32(2):213–21. https://doi.org/10.2355/isijinternational.32.213.

[18] Hwu YJ, Lenard JG. Phase Transformation Temperatures of an Ultra-Low

Carbon Steel. 1998.
[19] BS EN ISO 6892-1. Metallic materials - Part 1: Method of test at ambient. BSI. British Standards; 2009. https://doi.org/10.3403/30395181.
[20] Lee K, Han J, Park J, Kim B, Ko D. Prediction and control of front-end curvature in hot finish rolling process. Advances in Mechanical Engineering. 2015; 7(11). https://doi.org/10.1177/1687814015615043.
[21] Clyne TW, Campbell JE, Burley M, Dean J. Profilometry-Based Inverse Finite Element Method Indentation Plastometry. Advanced Engineering Materials. 2021; 23(9). https://doi.org/10.1002/adem.202100437.
[22] BS EN 10355:2013. Chemical analysis of ferrous materials — Inductively coupled plasma optical emission spectrometric analysis of unalloyed and low alloyed steels — Determination of Si, Mn, P, Cu, Ni, Cr, Mo and Sn, following dissolution with nitric and sulphuric acids, Routine method. 2013.
[23] Cheng YW, Tobler RL, Filla BJ, Coakley KJ. Constitutive Behavior Modeling of Steels Under Hot-Rolling Conditions. Boulder: 1999.
[24] Campbell JE, Zhang H, Burley M, Gee M, Fry AT, Dean J, et al. A Critical Appraisal of the Instrumented Indentation Technique and Profilometry-Based Inverse Finite Element Method Indentation Plastometry for Obtaining Stress–Strain Curves. Advanced Engineering Materials. 2021; 23(5). https://doi.org/10.1002/adem.202001496.